Journal of the Korean Society of Marine Environment & Safety
Research Paper
Vol. 24, No. 3, pp. 373-380, May 31, 2018, ISSN 1229-3431(Print) / ISSN 2287-3341(Online) https://doi.org/10.7837/kosomes.2018.24.3.373

A Study on Application of Electric Propulsion System using AFE Rectifier for Small Coastal Vessels

Hyeonmin Jeon* · Seongwan Kim** · Jongsu Kim***†
*, *** Division of Marine System Engineering, Korea Maritime and Ocean University, Busan 49112, Korea
** Man Diesel & Turbo Korea, Busan 46754, Korea

Abstract : *The small coastal vessel registered in Korea, small coastal vessels with a gross tonnage of 10 tons or less account for 94.6 % and among them, aged vessels over 16 years age indicate 40.6 %. In order to reduce GHG emissions from small coast vessels, discussions are underway to replace aging ships' propulsion units with eco - friendly propulsion facilities, and the electric propulsion ship is emerging as one of the measures. The electric propulsion system using the DFE rectifier, which was applied in the conventional large commercial vessel, was effective in reducing the harmonics and improving the DC output voltage of the DC link stage, but it occupied a large volume and caused an increase in the overall system price. Therefore, in this paper, we propose an electric propulsion system using AFE rectifier with a small volume of system that can be applied to a small coastal vessel. In order to analyze the effectiveness of the overall system, the load profile was applied to obtain accurate and rapid speed tracking performance of the propulsion motor affected by the speed load. In addition, the power factor and total harmonic distortion factor of the voltage and current on the improved power output side are derived through simulation.*

Key Words : *Small Coastal Vessels, Electric Propulsion Ship, Diode Front End (DFE), Active Front End (AFE), Load Profile*

1. Introduction

In the 72nd session of the Marine Environment Protection Committee (MEPC 72) meeting, which was held recently at the International Maritime Organization (IMO), attendees decided to reduce greenhouse gas emissions from international sailing vessels by at least 50 % of the total emissions by 2050. Republic of Korea is also influenced by the Paris Climate Agreement that came into effect in November 2015 and has revised the long-term national greenhouse gas reduction target; according to the Enforcement Decree of Framework Act on Low Carbon, Green Growth, it should be reduced to 37 % of the greenhouse gas emission estimate for 2030 (GGIRC, 2016; Kim et al., 2009).

According to the statistics of Ministry of Maritime Affairs and Fisheries, there are 66,067 small coastal vessels registered in Korea, of which 62,477 (94.6 %) are small coastal vessels weighing 10 tons or less. Of these, 26,800 vessels are 16 years old or older, which accounts for 40.6 %. According to the National Greenhouse Gas Inventory Report for 2016, greenhouse gas emissions of coastal shipping account for 1.1 % of the total greenhouse gas emissions for transportation. To reduce greenhouse gas emissions from coastal shipping, there have been active discussions on eco-friendly propulsion systems to replace aged small coastal vessels.

In the electric propulsion system using a Diode Front End (DFE) rectifier, which is widely used in conventional commercial vessel, a phase shifting transformer is installed to reduce the harmonics of generator output; however, this greatly increases the volume of the entire system and the cost, thus making it difficult to apply to small coastal vessels. On the other hand, when the electric propulsion system using an Active Front End (AFE) rectifier is applied, the total volume of the system is considerably reduced because the phase shifting transformer is not required. It is also possible to make sinusoidal wave of the input current in the power source supplied from the generator by controlly the rectifier (Zahedi, 2014; Ericsen et al., 2006).

Furthermore, this system can reduce the harmonics in the input signal, which significantly affects the quality of the generated power from the vessel. It has the advantage that the power factor of the input voltage and input current can be adjusted to the unit power factor (Li et al., 2010; Haresh and Ankit, 2016).

In this paper, therefore, an electric propulsion system using an AFE rectifier that is suitable for small coastal vessels is

* First Author : jhm861104@gmail.com, 051-410-4831
† Corresponding Author : jongskim@kmou.ac.kr, 051-410-4831

proposed. To analyze the validity of the overall system, the command speed values of the propulsion motor were predefined as low-, medium-, and high-speed regions. Thus, the accurate and rapid speed tracking of the propulsion motor, which is affected by the speed load, and the result of improved the total harmonic distortion factor and power factor can be derived through simulations.

2. The Rectifier of Electric Propulsion System

2.1 DFE rectification using phase shifting transformer

Harmonics are generated during ON/OFF control in the electric power conversion system of electric propulsion system; the generated harmonics are the main cause of quality deterioration of the power generation system of the vessel. To improve the quality degradation of an on-board power system due to harmonics, a phase shifting transformer is installed in the output of the generator. When the alternating current having a phase difference between the primary side and the secondary side is rectified, direct-current output waveforms in a DC link, which consists of multi-pulse, such as 12-pulse, 18-pulse, and 24-pulse, can be obtained (Wu, 2006).

Fig. 1 shows a block diagram of a 12-pulse rectifier using a typical phase shifting transformer; the quality of the DC output waveform and harmonic characteristics have been improved in comparison to the 6-pulse rectifier without a phase shifting transformer, and the phase-shift angle to generate the 12-pulse is 30° between the two waveforms.

$$\Delta = \angle V_{\overline{AB}} - \angle V_{ab} = 30^\circ \quad (1)$$

Where Δ is the phase shifting angle, V_{ab} is the primary line voltage and $V_{\overline{AB}}$ is the secondary line voltage

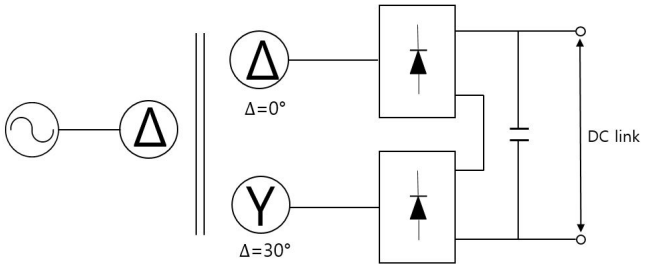

Fig. 1. Circuit diagram of 12-pulse diode rectifier.

2.2 AFE rectification using power semiconductor

The AFE rectifier uses a power semiconductor that can provide ON/OFF control. The rectifier consists of three stages, and two switches are connected in series at each stage as shown in Fig. 2. Moreover, an inductor that adjusts the magnitude of the input current is placed at the input terminal of the rectifier, and a capacitor is placed at the output terminal of the rectifier to maintain a constant DC output voltage.

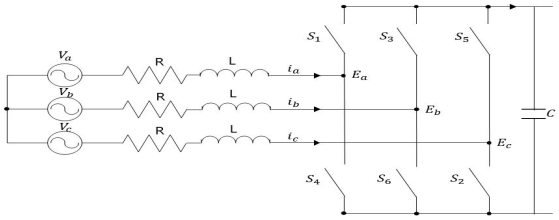

Fig. 2. Circuit diagram of AFE rectifier.

2.3 Harmonic generation of conventional rectifiers

The conventional rectifier can be divided into a diode rectifier, which cannot perform ON/OFF control, and the AFE rectifier, which consists of a power semiconductor that can perform switching control (Vasquez, 2014). The diode rectifier has DC output of a multi-pulse shape, such as 12-pulse, 18-pulse, or 24-pulse, depending on the connection method of a phase shifting transformer. IEEE Std519-2014 states the limit of the total harmonic distortion factor in the generator output voltage, and the result is shown in Table 1.

Table 1. Limitation of Total harmonic distortion

Voltage at PCC	Total harmonic distortion [%]
V ≤ 1.0kV	8.0
1.0kV < V ≤ 69kV	5.0
69kV < V ≤ 161kV	2.5
161kV < V	1.5

The total harmonic distortions in the generator outputs by using a conventional DFE rectifier and an AFE rectifier are shown in Table 2. Since 6-pulse rectification without a phase shifting transformer and 12-pulse rectification with a phase shifting transformer are not compatible with the IEEE standard, different harmonic improvement measures should be applied. Although the total harmonic distortion factors can be obtained in 18- and 24-pulse, to improve the harmonics, internal connections

are difficult to make properly to generate a phase difference in the phase shifting transformer, and the volume and weight will increase. For an AFE rectifier, in which a phase shifting transformer is not installed, excellent rectification performance can be obtained, including DC output waveform and excellent total harmonic distortion factor through switching control of a power semiconductor; however, it is necessary to accurately measure the phase angle of the power supply voltage for the rectifier control.

Table 2. Comparison of Total harmonic distortion

Rectifier Classification	Total harmonic distortion [%]
6 Pulse	25 ~ 27
12 Pulse with PST	8 ~ 11
18 Pulse with PST	4 ~ 5
24 Pulse with PST	2 ~ 3
AFE	4 ~ 5

* PST: Phase Shifting Transformer

3. Electric Propulsion System using the proposed AFE Rectifier

3.1 AFE rectifier

Fig. 3 shows the basic structure of a 3-phase AC in AFE rectifier. It consists of three stages and 6 switches, which are supplied with 3-phase AC power signals of v_a, v_b and v_c. The inductors positioned at the power output of the generator is used for controlly amplitude of AC current i_a, i_b and i_c supplied to the rectifier, and the capacitor positioned at the rectifier output is used to smooth the DC voltage at the DC link terminal.

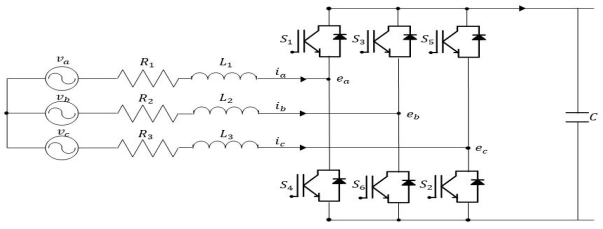

Fig. 3. Circuit diagram of proposed AFE rectifier.

$$v_a + v_b + v_c = 0 \tag{2}$$

$$i_a + i_b + i_c = 0 \tag{3}$$

The voltage equation of the AFE rectifier is as follows

$$v_{abc} = Ri_{abc} + L\frac{di_{abc}}{dt} + e_{abc} \tag{4}$$

Where v_{abc} is the power supply, i_{abc} is the phase current and e_{abc} is the input voltage of rectifier

To obtain the current value in phase the supply voltage with the d-q axis conversion, which facilitates switching control of the 3-phase AFE rectifier, it is necessary to detect the control phase angle θ corresponding to the real phase angle. As shown in Fig. 4 the proposed phase controller converts the power supply voltage into a synchronous rotational coordinate system d-q axis to generate DC voltage values v_d, v_q. It arbitrarily sets the active power to v_d, sets the reactive power to v_q, and controls the voltage value of v_q to zero.

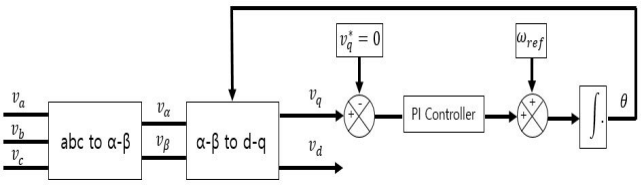

Fig. 4. Block diagram of proposed Phase angle controller.

The relationship between the phase angle for making the voltage value of the reactive power v_q to 0 and the q-axis voltage of the synchronous rotational coordinate system is shown in Fig. 4, where P_s in Equation (5) is the supply active power.

$$P_s = v_a i_a + v_b i_b + v_c i_c = \frac{3}{2}(v_d i_d + v_q i_q) = \frac{3}{2} v_d i_d \tag{5}$$

Since the voltage of the reactive power v_q is controlled to zero, it can be neglected in Equation (5). Also, since the equation is influenced only by the voltage value of the active power v_d the supply power becomes $P_s = \frac{3}{2} v_d i_d$. Therefore, if the effective power is set to the d-axis and the reactive power of the q-axis is set to zero, then the real phase angle θ matches the control angle $\hat{\theta}$ as shown in Fig. 5. Thus, the phase angle θ can be obtained accurately.

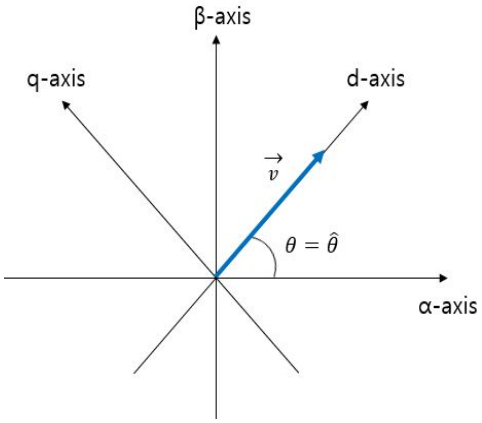

Fig. 5. The match of Real phase angle and Control phase angle.

Since it is possible to control the reactive q-axis voltage to zero even at irregular outputs including harmonics and noise when the phase is detected by using the proposed phase controller, the phase angle θ that corresponds to the real phase can be found and controlled. Thus, the supply voltage and current become unit power factor in the same phase.

$$PF = \frac{i_d}{\sqrt{i_d^2 + i_q^2}} \tag{6}$$

In Equation (10), if the reactive power component of v_q on the synchronous rotational coordinate system is adjusted to zero its value becomes zero, then $\theta = \hat{\theta}$, and the effective power component v_d becomes V. Thus, the imaginary phase angle $\hat{\theta}$ is controlled to have the same value as the real phase angle θ. Fig. 6 shows a block diagram of an improved phase-angle controller using a proportional integral controller.

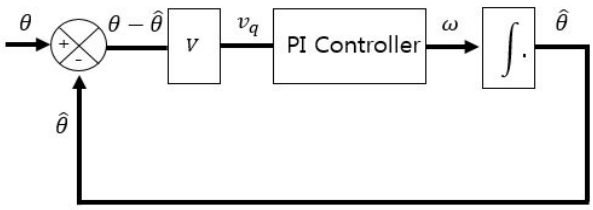

Fig. 6. Block diagram of proposed phase angle controller.

$$v_d = v_\alpha \cos\hat{\theta} + v_\beta \sin\hat{\theta} \tag{7}$$

$$v_q = -v_\alpha \sin\hat{\theta} + v_\beta \cos\hat{\theta} \tag{8}$$

$$v_d = V(\cos\theta\cos\hat{\theta} + \sin\theta\sin\hat{\theta}) = V\cos(\theta - \hat{\theta}) \tag{9}$$

$$v_q = V(-\cos\theta\sin\hat{\theta} + \sin\theta\cos\hat{\theta}) = V\sin(\theta - \hat{\theta}) \tag{10}$$

3.2 Speed control of propulsion motor

The indirect vector control calculates the slip-command angular velocity using the flux current, torque current, and motor constant in the synchronous rotational coordinate system. This value is then added to the rotor speed to compute the integral, and the resulting value is used to estimate the magnetic flux angle. For high-performance torque and flux control, the stator current supplied to the motor should be controlled by categorization of the current into components that are orthogonal to the reference flux and that are same as the reference flux. The indirect vector control based on the rotor flux selects the synchronous angular speed so that the instantaneous speed becomes the same as the rotor speed, and the rotating magnetic flux exists only on the d-axis.

As shown in Fig. 7 the α-β axis is fixed to a stator; the d-q axis rotates at the synchronous angular velocity ω_e, the rotating axis of the rotor is made to be the same as the d-axis; and the slip angle θ_{sl} to the rotor axis is maintained at a constant value. Therefore, it can be seen that the stator current supplied to the motor is separated into the magnetic flux component current i_{ds} and the torque component current i_{qs} and it is controlled for high-performance torque and magnetic flux control.

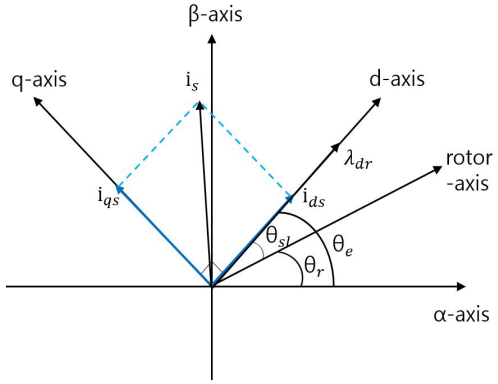

Fig. 7. Vector diagram of indirect field oriented control.

The indirect vector control based on the rotor flux is applied so that the rotor flux exists only in the d-axis component; therefore, Equation (11) is valid.

$$\lambda_{qr} = \rho\lambda_{qr} = 0 \tag{11}$$

The torque equation is given by the following (12).

$$T_e = \frac{3}{2}\frac{P}{2}\frac{L_m}{L_r}\lambda_{dr} i_{qs} \tag{12}$$

As shown in Equation (12), because the torque is proportional to i_{qs}, i_{qs} is the torque component current. Also, in the case of constant flux control, the rotor flux can be controlled by i_{ds} and i_{ds} is the flux component current.

Therefore, the slip relationship equation can be expressed by Equation (13) as follows:

$$\omega_{sl} = \frac{R_r}{L_r}\frac{i_{qs}}{i_{ds}} \tag{13}$$

Since the position of the rotor flux is the integral of the motor speed and the slip command angular speed, Equation (14) can be obtained.

$$\theta_e = \int (\omega_r + \omega_{sl})dt \tag{14}$$

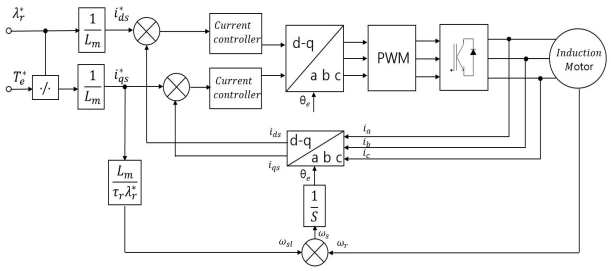

Fig. 8. Block diagram of indirect field oriented control.

4. Simulation

Fig. 9 shows a schematic diagram of the entire electric propulsion system for small coastal vessels proposed in this paper. In the rectifier stage, the proposed AFE rectifier is applied, and in the inverter stage, the entire system is constructed using a propulsion motor controller with an indirect vector control method.

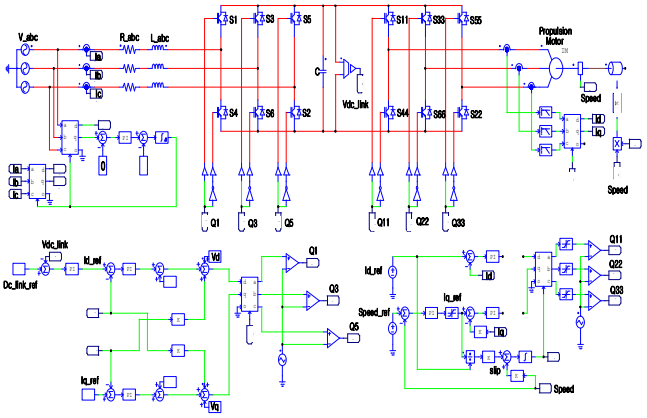

Fig. 9. Circuit diagram of proposed Electric Propulsion System.

The parameter constants of the circuit design presented in Fig. 9 are shown in Table 3, and the parameter constants of the propulsion motor are shown in Table 4.

Table 3. Parameter for circuit

Input Voltage	440 [V]
Frequency	60 [Hz]
Capacitor	3000 [㎌]
Switching Frequency	10 [kHz]

Table 4. Parameter for Propulsion motor

Rated Output	290 [kW]
Pole	10
Rated Speed	650 [rpm]
Stator Resistance	0.01002 [Ω]
Stator Inductance	0.1525 [H]
Rotor Resistance	0.01351 [Ω]
Rotor Inductance	0.16602 [H]
Mutual Inductance	5.2042 [H]
Moment of inertia	6.3863 [kg·㎡]

Furthermore, the effectiveness of the proposed electric propulsion system for the speed control of the propulsion motor was assessed in relation to variation of the speed load. For this purpose, the load power profiles of the propulsion system of a small coastal vessel were In port, Maneuvering, Sea going, and Drifting modes, as shown in Fig. 10 and results were obtained by simulation.

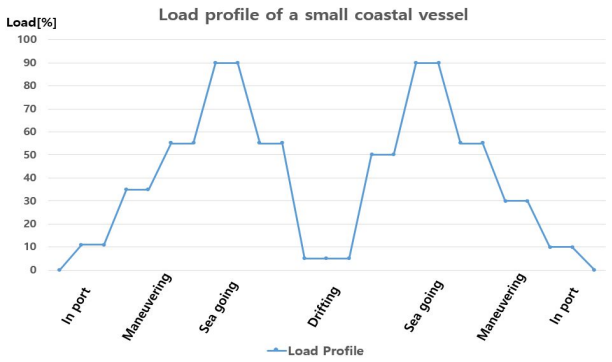

Fig. 10. Load profile of small coastal vessel for Electric Propulsion System.

In order to verify the effectiveness of the speed control of the propulsion motor according to the change of the speed load, the profiles of the propulsion power that was used in Fig. 10—In port, Maneuvering, Sea going, and Drifting—were also used in Fig. 11 to conduct simulation, and the results show that the rapid speed control of the propulsion motor was observed at the change of the speed load.

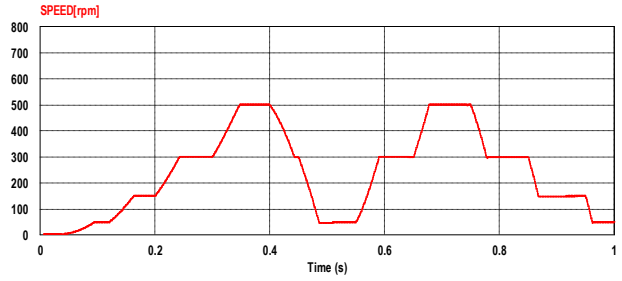

Fig. 11. Simulation responses for step change as load profile.

Fig. 12 shows the simulation results of the speed response of the propulsion motor for the step speed command at 50 [rpm], 150 [rpm], 300 [rpm] and 500 [rpm]. The results indicate that the speed control characteristic accurately follows the speed of the propulsion motor in a short time according to the given speed command value.

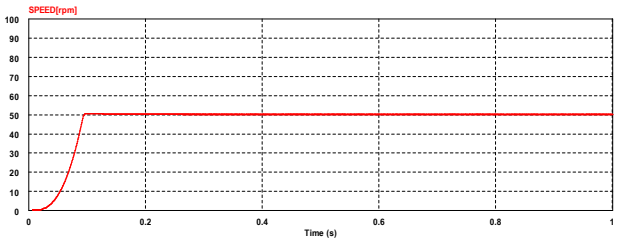

(a) Reference : 50 [rpm]

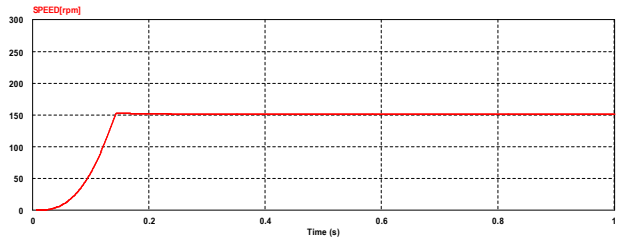

(b) Reference : 150 [rpm]

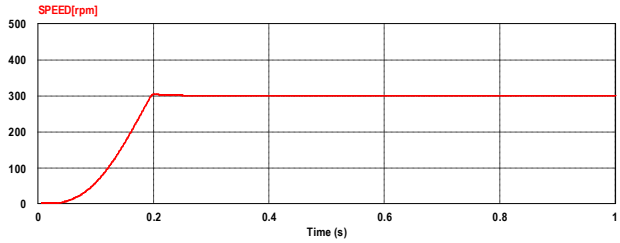

(c) Reference : 300 [rpm]

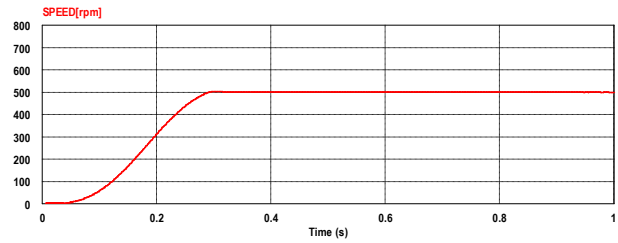

(d) Reference : 500 [rpm]

Fig. 12. Simulation responses for step change of speed reference.

Fig. 13 shows the magnitude and phase of the voltage and current according to the speed of the propulsion motor in the electric propulsion system using the proposed AFE rectifier; the voltage and current are in phase, resulting in a sinusoidal output with a unit power factor and little noise.

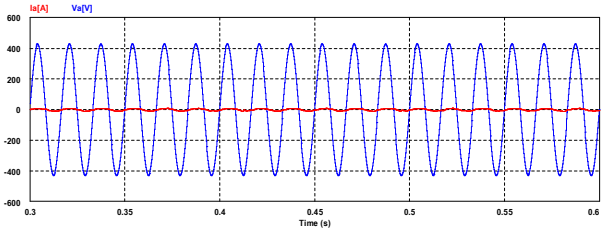

(a) Reference : 50 [rpm]

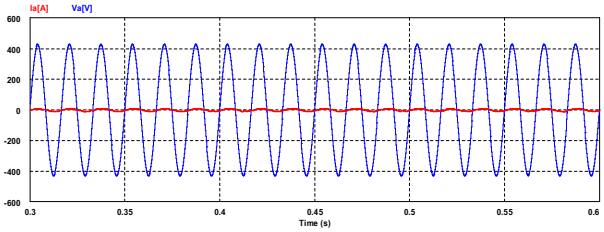

(b) Reference : 150 [rpm]

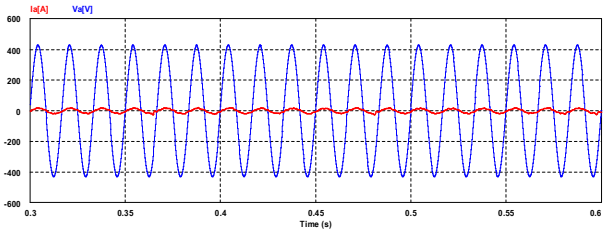

(c) Reference : 300 [rpm]

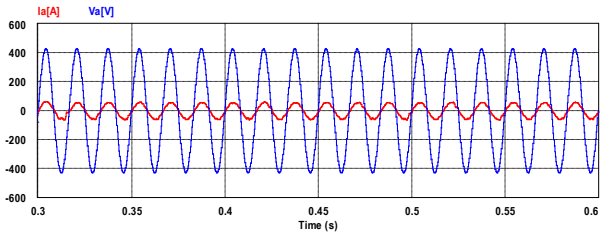

(d) Reference : 500 [rpm]

Fig. 13. Power factor for input voltage and current of proposed Electric Propulsion System.

Fig. 14 shows the result of the total harmonic distortion factor in the generator output, and its value is about 2.5 %, which satisfies the reference value of 8 % specified in IEEE Std519-2014.

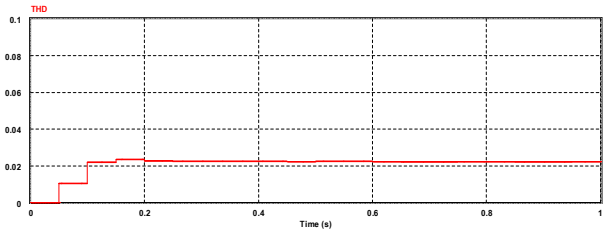

(a) Reference : 50 [rpm]

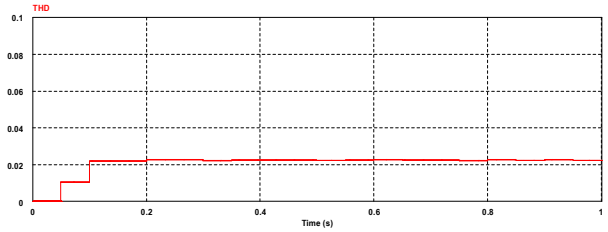

(b) Reference : 150 [rpm]

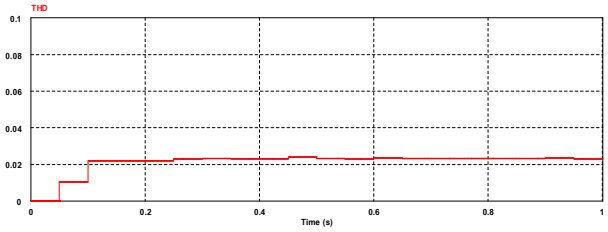

(c) Reference : 300 [rpm]

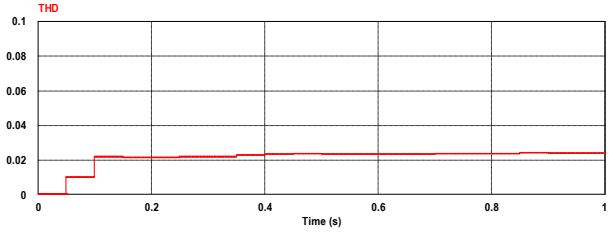

(d) Reference : 500 [rpm]

Fig. 14. Total harmonic distortion for proposed Electric Propulsion System.

5. Conclusion

To calculate the phase angle, which is an essential factor for accurate control of the proposed AFE rectifier, a phase detection circuit for a power supply voltage was applied, and the propulsion motor was simulated by constructing a small electric propulsion system using an indirect vector control method. The load operation characteristics in relation to the speed load were analyzed by categorization of the speed command value of the propulsion motor into the low-, middle-, and high-speed regions.

Simulation results of the propulsion load power profile of a small coastal vessel show that the propulsion motor follows the speed command value rapidly even when the speed command and load are varied. Therefore, it was demonstrated that stability and quick response of the small vessel propulsion system using the proposed AFE rectifier are excellent.

Acknowledgements

This research was supported by the Korea Institute of Marine Science & Technology Promotion (KIMST) grant funded by the Ministry of Oceans and Fisheries in 2018 (NO 20180066).

References

[1] Ericsen, T., N. Hingorani and Y. Khersonsky(2006), Power electronics and future marine electrical systems, IEEE Trans, Vol. 42, pp. 155-163.

[2] Greenhouse Gas Inventory and Research Center(2016), National Greenhouse Gas Inventory Report of Korea.

[3] Haresh, P. and S. Ankit(2016), A novel control method for UPS battery charging using Active Front End (AFE) PWM rectifier, IEEE Power Electronics Drives and Energy Systems, pp. 978-980.

[4] Kim, B. J, W. S. Kim, U. S. Kim, C. H. Kim and G. S. Kim(2009), Response to the Convention on Climate Change in the Port Area, Korea Maritime Institute.

[5] Li, Y. W., M. Pande, N. Zargari and W. Bin(2010), An input power factor control strategy for high-power current-source induction motor drive with active front-end, IEEE Transactions Power Electron, Vol. 25(2), pp. 352-359.

[6] Vasquez, C.(2014), A methodology to select the electric propulsion system for Platform Supply Vessels, Sao Paulo University.

[7] Wu, B.(2006), High-Power Converters and AC Drives, 2nd Edition, John Wiley & Sons, pp. 37-64.

[8] Zahedi, B.(2014), Shipboard DC Hybrid Power Systems, Norwegian University of Science and Technology.

Received : 2018. 05. 11.
Revised : 2018. 05. 27.
Accepted : 2018. 05. 29.